Phosphinobenzyl- and Aryl-silanes and Their Triosmium Cluster Carbonyl Derivatives *

How Ghee Ang, Betty Chang and Whei Lu Kwik
Department of Chemistry, National University of Singapore, Lower Kent Ridge Road, 0511 Singapore

The Grignard reagents MgR(Br) (R = $C_6H_4CH_2SiMe_2H$-*o* or $C_6H_4CH_2SiMeH_2$-*o*) have been found to undergo unusual reactions with Ph_2PCl to afford *o*-$Ph_2PC_6H_4CH_2SiMe_2H$ **I** and *o*-$HMe_2SiC_6H_4CH_2PPh_2$ **II** and *o*-$Ph_2PC_6H_4CH_2SiMeH_2$ **III** and *o*-$H_2MeSiC_6H_4CH_2PPh_2$ **IV** respectively. Reactions of the respective bidentate ligands **I**, **II**, **III** and **IV** with $[Os_3(CO)_{10}(MeCN)_2]$ gave the novel triosmium clusters $[Os_3(\mu\text{-}H)(CO)_{10}(L\text{–}L)]$ **1**, **2**, **3** and **4** involving cleavage of one Si–H bond. Similar reactions of ligands **II** and **IV** with $[Os_3(\mu\text{-}H)_2(CO)_{10}]$ afforded two new clusters $[Os_3(\mu\text{-}H)_3(CO)_8(L\text{–}L)]$ **5** and **6** respectively. The structures of **1**, **2**, **4** and **5** have been determined by single-crystal X-ray diffraction techniques. In each case, the ligand assumes a chelating mode across the long edge of the osmium triangle which is also bridged by a hydride. The high-performance liquid chromatographic behaviour of these clusters has also been determined and correlated with the size and nature of the ligands.

Whereas the reactivity of substituted phosphines and chelating diphosphines towards triosmium clusters has been extensively studied,[1,2] relatively few triosmium clusters with ligands containing silicon as donor atom have been reported.[3–6] Recently, triosmium clusters, *viz.*, $[Os_3H(CO)_{10}\{Si(OEt)_3\}(dppe)]$ [dppe = 1,2-bis(diphenylphosphino)ethane] and $[Os_3H(CO)_{10}\{Si(OMe)_3\}_2(\mu\text{-dppe})]$ containing both osmium–silicon and –phosphorus bonds have been reported.[7] It is of further interest that the bidentate ligands phosphinoethylsilanes $Ph_2PCH_2CH_2SiR^1R^2H$ ($R^1 = R^2$ = Me or Ph; R^1 = Me, R^2 = Ph) have been reported to react with $[Os_3(CO)_{12}]$ to afford mononuclear octahedral complexes $[Os(CO)_2(PPh_2CH_2CH_2SiR^1R^2)_2]$.[8]

We report here the unusual reactions of the Grignard reagents MgR(Br) (R = $C_6H_4CH_2SiMe_2H$-*o* or $C_6H_4CH_2SiMeH_2$-*o*) with Ph_2PCl and the co-ordinating properties of the derived products with triosmium carbonyl clusters.

Results and Discussion

Synthesis of Ligands.—The ligand pairs (*a*) *o*-$Ph_2PC_6H_4CH_2SiMe_2H$ **I** and *o*-$HMe_2SiC_6H_4CH_2PPh_2$ **II** and (*b*) *o*-$Ph_2PC_6H_4CH_2SiMeH_2$ **III** and *o*-$H_2Me_2SiC_6H_4CH_2PPh_2$ **IV** were obtained from reactions involving the addition of Ph_2PCl at 0 °C to the Grignard reagents *o*-$BrMgC_6H_4CH_2SiMe_2H$ and *o*-$BrMgC_6H_4CH_2SiMeH_2$ respectively, according to equation (1) (*n* = 1, **I** and **II**; *n* = 2, **II** and **IV**). Separations of

$$o\text{-}BrMgC_6H_4CH_2SiMe_{3-n}H_n + Ph_2PCl \longrightarrow o\text{-}Ph_2PC_6H_4CH_2SiMe_{3-n}H_n + o\text{-}H_nMe_{3-n}SiC_6H_4CH_2PPh_2 \quad (1)$$

I/**II** and of **III**/**IV** were not achieved as the two isomers from the same Grignard reaction distilled in the same temperature ranges of 175–180 °C and of 178–180 °C respectively during bulb-to-bulb distillation at a pressure of 0.01 mmHg. The formation of pairs of these ligands was first revealed from a careful analysis of the ^1H, ^{31}P and ^{29}Si (Table 1) NMR spectra. Thus, the ^1H NMR spectra displayed two sets of signals for each type of protons which could be assigned to **I** and **II** as follows: δ 7.29 (m, C_6H_5, C_6H_4 of **I** + **II**), 4.650 (m, SiH, **II**), 3.96 (m, SiH, **I**), 3.58 (s, CH_2, **II**), 2.47 (d, CH_2, **I**), 0.34 (d, CH_3, **II**) and 0.076 (d, CH_3, **I**). In addition, there are two signals each observed in the ^{31}P NMR spectrum (δ −9.02 due to **II** and at −14.235 due to **I**) as well as in the ^{29}Si NMR spectrum (δ −10.61 due to **II** and at −10.78 due to **I**). In all three spectra the relative intensities of the two sets of signals suggest that **I** and **II** were formed in approximately 1:2 ratio. Similar patterns of ^1H, ^{31}P and ^{29}Si NMR spectral data (Table 1) are found for **III** and **IV**. The formation of pairs of these isomers is similar to that reported by de Boer, *et al.*[9] where the Grignard reagent *o*-$BrMgC_6H_4CH_2SnMe_3$ has been found to undergo rearrangement to *o*-$Me_3SnC_6H_4CH_2MgBr$. Subsequent reactions with $GeMe_3Cl$ then gave the products *o*-$Me_3GeC_6H_4CH_2SnMe_3$ and *o*-$Me_3SnC_6H_4CH_2GeMe_3$.

Table 1 Infrared (cm^{-1}) and NMR data in $CDCl_3$ for the ligands **I**/**II** and **III**/**IV**

I/**II**	IR	3052s, 3000m, 2956s, 2899w, 2123vs, 1586s, 1559w, 1477s, 1433vs, 1249s, 1203vs, 1158m, 1123s, 1069m, 1027m, 999w, 946s, 886vs, 838s, 776s, 742vs, 696vs, 506s, 473m, 429m
	δ_H	0.076 (d, CH_3, **I**), 0.335 (d, CH_3, **II**), 2.467 (d, CH_2, **I**), 3.582 (s, CH_2, **II**), 3.965 (m, SiH, **I**), 4.650 (m, SiH, **II**), 7.294 (m, C_6H_4, C_6H_5, **I**/**II**)
	δ_P	−14.235 (**I**), −9.019 (**II**); δ_{Si} −10.779 (**I**), −10.614 (**II**)
III/**IV**	IR	3052s, 3000m, 2961w, 2905w, 2137vs, 1585s, 1560w, 1477s, 1432vs, 1251s, 1198m, 1158m, 1110s, 1069m, 1026m, 999w, 947s, 894vs, 822m, 773s, 741vs, 695vs, 506s, 473m, 428m
	δ_H	0.100 (t, CH_3, **III**), 0.403 (t, CH_3, **IV**), 2.523 (t, CH_2, **III**), 3.547 (s, CH_2, **IV**), 3.839 (m, SiH, **III**), 4.407 (q, SiH, **IV**), 7.156 (m, C_6H_4, C_6H_5, **III**/**IV**)
	δ_P	−13.999 (**III**), −9.154 (**IV**); δ_{Si} −41.14 (**III**), −40.93 (**IV**)

Reactions of $[Os_3(CO)_{10}(MeCN)_2]$ *with Ligands* **I**/**II** *and* **III**/**IV**.—When dichloromethane solutions of **I**/**II** and **III**/**IV** were allowed to react with $[Os_3(CO)_{10}(MeCN)_2]$ in evacuated reaction tubes at room temperature, the clusters **1** and **2** and **3** and **4** respectively were obtained. Pairs of these clusters were

* *Supplementary Data available:* see Instructions for Authors, *J. Chem. Soc., Dalton Trans.*, 1992, Issue 1, pp. xx–xxv.

Non-SI unit employed: mmHg ≈ 133 Pa.

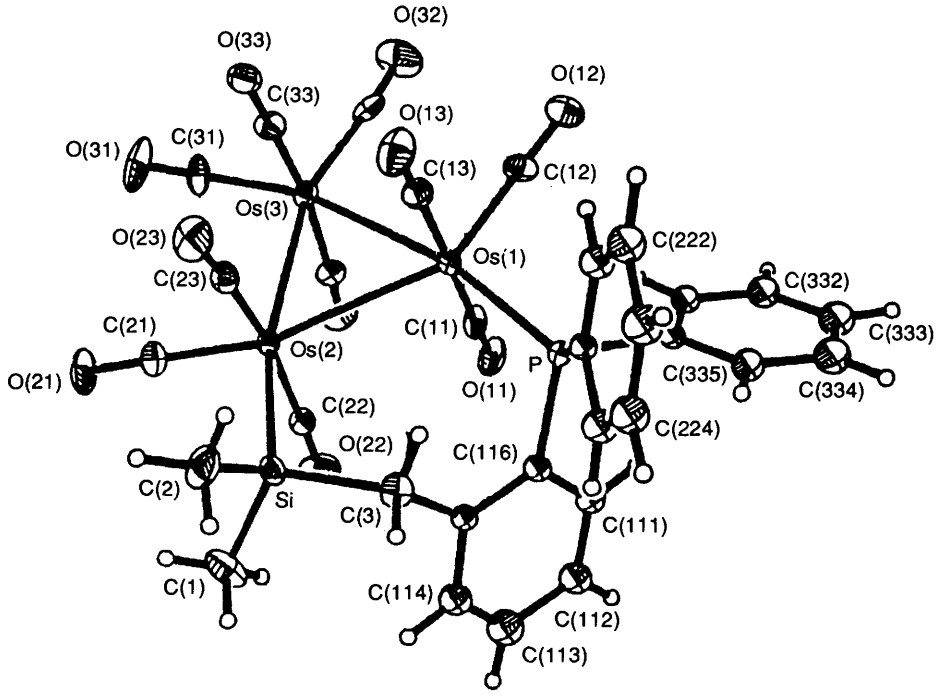

Fig. 1 The molecular structure of $[Os_3(\mu\text{-}H)(CO)_{10}(o\text{-}Ph_2PC_6H_4CH_2SiMe_2)]$ **1** showing the atom labelling

Table 2 Infrared in cyclohexane (cm^{-1}) and NMR data in $CDCl_3$ (J/Hz) for the complexes

1 $[Os_3(\mu\text{-}H)(CO)_{10}(o\text{-}Ph_2PC_6H_4CH_2SiMe_2)]$

ν_{CO} 2102m, 2057ms, 2037s, 2017vs, 2008m, 1995m, 1978m
δ_H −19.195 (d, OsHOs, J_{PH} 12.46), 0.743 (s, CH_3), 2.812 (m, CH_2), 6.968 (m, C_6H_5, C_6H_4); δ_P −1.884

2 $[Os_3(\mu\text{-}H)(CO)_{10}(o\text{-}Me_2SiC_6H_4CH_2PPh_2)]$

ν_{CO} 2103m, 2059s, 2036s, 2021vs, 2006ms, 1995s, 1980m, 1962w
δ_H −19.490 (d, OsHOs, J_{PH} 13.92), 1.021 (s, CH_3), 4.544 (m, CH_2), 7.205 (m, C_6H_5, C_6H_4); δ_P −9.826

3 $[Os_3(\mu\text{-}H)(CO)_{10}(o\text{-}Ph_2PC_6H_4CH_2SiMeH)]$

ν_{CO} 2104w, 2057m, 2038m, 2018vs, 2008m, 1996s, 1980m

4 $[Os_3(\mu\text{-}H)(CO)_{10}(o\text{-}HMeSiC_6H_4CH_2PPh_2)]$

ν_{CO} 2104mw, 2058m, 2038ms, 2021s, 2007m, 1996ms, 1981m
δ_H −19.719 (d, OsHOs, J_{PH} 13.91), 1.083 (d, CH_3), 4.499 (m, CH_2), 5.689 (m, SiH), 6.812 (m, C_6H_5, C_6H_4); δ_P −8.750

5 $[Os_3(\mu\text{-}H)_3(CO)_8(o\text{-}Me_2SiC_6H_4CH_2PPh_2)]$

ν_{CO} 2102m, 2057ms, 2037s, 2107vs, 2008m, 1995m, 1978m
δ_H −12.702 (s, OsHOs, J_{PH} 14.65), −11.615 (s, OsHOs), −7.895 (s, OsHOs), 1.201 (s, CH_3), 2.513 (d, CH_2), 7.009 (m, C_6H_5, C_6H_4); δ_P −3.500

6 $[Os_3(\mu\text{-}H)_3(CO)_8(o\text{-}HMeSiC_6H_4CH_2PPh_2)]$

ν_{CO} 2091m, 2057m, 2026s, 2011s, 1997ms, 1964m
δ_H −12.628 (s, OsHOs, J_{PH} 15.38), −11.864 (s, OsHOs), −8.002 (s, OsHOs), 0.224 (d, CH_3), 2.198 (m, CH_2), 4.620 (m, SiH), 7.049 (m, C_6H_5, C_6H_4); δ_P −4.173

separated by TLC using 10% CH_2Cl_2 in hexane as eluent. However $[Os(\mu\text{-}H)(CO)_{10}(o\text{-}Ph_2PC_6H_4CH_2SiMeH)]$ **3** was found to be very unstable. The ^1H, ^{29}Si and ^{31}P NMR spectral data for **1**, **2** and **4** as well as the IR data for **1**–**4** are in Table 2. Cluster **1** was crystallised from a hexane solution, whereas **2** and **4** were crystallised from a mixture of dichloromethane and hexane.

All four compounds display distinct absorptions at *ca.* 2103, 2058, 2038, 2020, 2007, 1995 and 1980 cm^{-1}, similar to carbonyl stretchings for $[Os_3(CO)_{10}\{Si(OEt)_3\}(dppe)]$.[7] The IR data strongly suggest that the spatial arrangements of the ten carbonyls in the four clusters are similar.

The metal hydride resonances are found at δ −19.20, −19.49 and −19.72[10] for **1**, **2** and **4** respectively, indicative of a bridging hydride in each case. Moreover, each of these signals is split by the ^{31}P to give a doublet with a coupling constant of *ca.* 13 Hz. The methylene ^1H resonance of **1** is found at lower frequency than those of **2** and **4** presumably due to the shielding effect of the silicon to which this methylene group is linked in **1**. The $^{31}P\text{-}\{^1H\}$ NMR signals of **1**, **2** and **4** occur at δ −1.88, −9.84 and −8.75 respectively.

Structures of $[Os_3(\mu\text{-}H)(CO)_{10}(o\text{-}Ph_2PC_6H_4CH_2SiMe_2)]$ **1**, $[Os_3(\mu\text{-}H)(CO)_{10}(o\text{-}Me_2SiC_6H_4CH_2PPh_2)]$ **2**, *and* $[Os_3(\mu\text{-}H)(CO)_{10}(o\text{-}HMeSiC_6H_4CH_2PPh_2)]$ **4**.—The molecular structures of clusters **1**, **2** and **4** are shown in Figs. 1, 2 and 3 while the atomic coordinates are given in Tables 3–5 and the relevant bond lengths and angles in Tables 6–8. The Os–Os bonds in all cases are longer than the average Os–Os bond length of 2.877 Å of the parent carbonyl $[Os_3(CO)_{12}]$. The longest Os–Os bond in **1** [3.024(1)], **2** [3.019(1)] and **4** [3.036(1) Å] corresponds to that bridged by the chelating ligand and most likely the hydride as located by ^1H NMR spectroscopy. However, the Os–Os bond lengths found in **1**, **2** and **4** are comparable to those of the cluster $[Os_3(\mu\text{-}H)(CO)_{10}\{Si(OEt)_3\}(dppe\text{-}P)]$[1] in which the Os–Os bond lengths are 3.030, 2.924 and 2.890 Å. It would appear that the lengthening of the Os–Os bond in **1**, **2** and **4** in comparison to those of $[Os_3(CO)_{12}]$ is largely the effect of the bridging hydrides.

Although the Os–P distances of clusters **1** [2.360(3)], **2** [2.354(5)] and **4** [2.363(5) Å] are comparable to that of $[Os_3(\mu\text{-}H)(CO)_{10}\{Si(OEt)_3\}(dppe)]$, the Os–Si distances are relatively longer in the present series [2.444(4) for **1**, 2.453(5) for **2**, 2.425(7) for **4** and 2.400(4) Å for $[Os_3(\mu\text{-}H)(CO)_{10}\{Si(OEt)_3\}(dppe)]$. Such lengthening is most likely related to the chelating nature of the ligands in **1**, **2** and **4**, which has apparently affected the weaker Os–Si bond rather than the Os–P bond.

The silicon and phosphorus atoms are a little bent from their equatorial positions. Thus, the Os(3)–Os(2)–Si angles are 165.1(1), 158.8(1) and 159.5(1)° respectively for **1**, **2** and **4**. Similarly, the Os(3)–Os(1)–P angles are 165.2(1), 167.3(1)

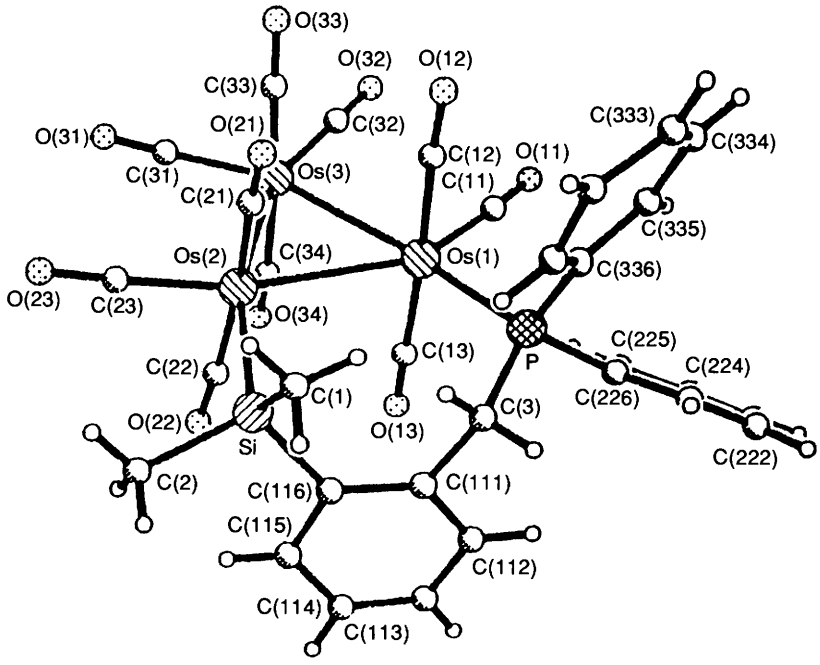

Fig. 2 The molecular structure of $[Os_3(\mu\text{-}H)(CO)_{10}(o\text{-}Me_2SiC_6H_4CH_2PPh_2)]$ **2** showing the atom labelling

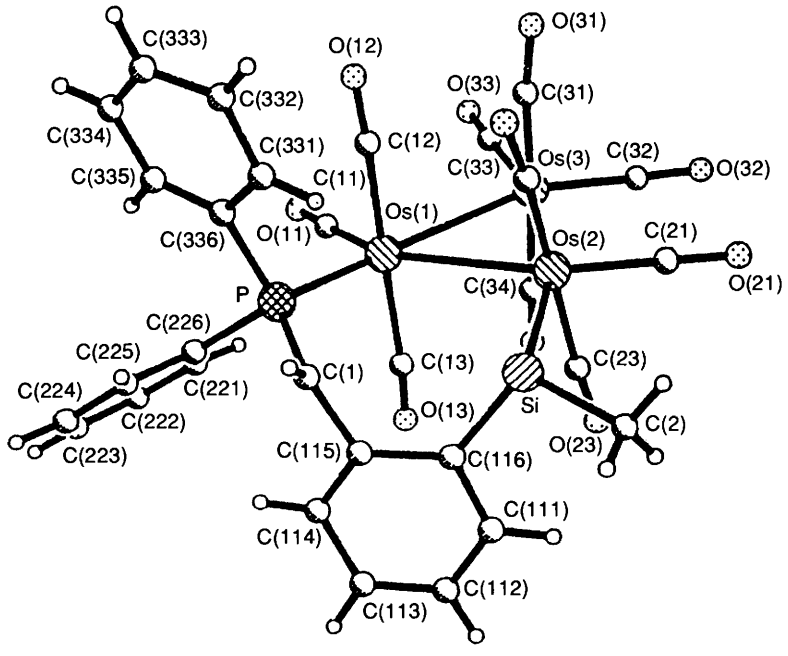

Fig. 3 The molecular structure of $[Os_3(\mu\text{-}H)(CO)_{10}(o\text{-}HMeSiC_6H_4CH_2PPh_2)]$ **4** showing the atom labelling

and 164.4(1)° respectively. It is also interesting that the Os(1)–Os(2)–Si angles [106.1(1), 102.9(1) and 102.1(1)°] as well as the Os(2)–Os(1)–P angles [111.0(1), 109.7(1) and 108.5(1)°] in the present series are all smaller than the corresponding ones [115.9(1) and 114.2(1)° respectively] reported for $[Os_3(\mu\text{-}H)(CO)_{10}\{Si(OEt)_3\}(dppe)]$. The chelating nature of the ligands **I**, **II** and **IV** together with the bulkiness of the dppe may have led to these differences.

The silicon and phosphorus atoms of the co-ordinated ligands in clusters **1**, **2** and **4** preserve their sp^3 hybridisation with the average Os(1)–P–C angle being 114.8, 115.2 and 115.5° and Os(2)–Si–C being 113.0, 110.1 and 112.6° respectively.

The ten carbonyls in clusters **1**, **2** and **4** are all essentially linear, the mean Os–C–O angles being 176.3(12), 175.5(18) and 175.2(12)°. The average Os–CO distances are 1.91, 1.92 and 1.90 Å, the the average C–O distances are 1.14, 1.13 and 1.14 Å.

Reactions of Ligands **I**/**II** *and* **III**/**IV** *with* $[Os_3(\mu\text{-}H)_2(CO)_{10}]$.—Reactions of the two sets of ligands **I**/**II** and **III**/**IV** with $[Os_3(\mu\text{-}H)_2(CO)_{10}]$ yielded, in each case, several products. Upon TLC separations two major products were identified for each system, *viz.* **2** and **5** for reaction with **I**/**II** and **4** and **6** for that with **III**/**IV**. Compound **5** was characterised by X-ray structural study to be $[Os_3(\mu\text{-}H)_3(CO)_8(o\text{-}Me_2SiC_6H_4CH_2PPh_2)]$ in which the ligand **II** bonds through both P and Si as in **2**. Since both **5** and **6** display very similar carbonyl stretchings at *ca.* 2090, 2058, 2024, 2010, 1995 and 1960 cm^{-1} it is most likely that **6** has a similar structure to that of **5**. It is also of interest that these carbonyl stretchings are distinctly different from those of $[Os_3(\mu\text{-}H)_3(CO)_9(SiPh_3)]$ and $[Os_3(\mu\text{-}H)_3(CO)_{10}(SiPh_2H)]$.[11]

Moreover, the ^1H NMR spectra of clusters **5** and **6** as given in Table 2 are remarkably similar. Three metal–hydride signals of equal intensity are observed at δ −12.70, −11.62 and −7.89

Table 3 Fractional atomic coordinates for $[Os_3(\mu\text{-H})(CO)_{10}(o\text{-}Ph_2PC_6H_4CH_2SiMe_2)]$ with standard deviations in parentheses

Atom	x	y	z	Atom	x	y	z
Os(1)	939(1)	5 427(1)	2 409(1)	O(32)	−2 820(13)	5 996(13)	1 091(10)
Os(2)	2 847(1)	7 794(1)	2 633(1)	O(33)	1 012(18)	7 056(16)	14(9)
Os(3)	70(1)	7 336(1)	1 847(1)	O(34)	−658(15)	7 825(17)	3 662(10)
P	2 121(4)	4 135(3)	2 843(3)	C(111)	3 697(18)	5 595(16)	4 439(12)
Si	4 821(5)	7 617(4)	3 603(3)	C(112)	3 089(18)	5 033(17)	5 154(11)
C(11)	−805(21)	4 402(13)	2 044(12)	C(113)	3 105(20)	5 698(19)	5 947(11)
C(12)	1 312(20)	5 188(14)	1 213(12)	C(114)	3 642(25)	6 797(23)	6 048(14)
C(13)	626(16)	5 759(14)	3 636(11)	C(115)	4 220(18)	7 396(17)	5 348(12)
C(21)	3 604(18)	7 451(16)	1 576(13)	C(116)	4 213(16)	6 767(15)	4 522(10)
C(22)	2 401(17)	8 283(13)	3 783(14)	C(221)	1 837(23)	2 061(18)	3 496(14)
C(23)	3 541(22)	9 358(16)	2 568(16)	C(222)	1 113(23)	1 136(19)	3 856(14)
C(31)	118(20)	8 859(18)	1 687(14)	C(223)	−167(21)	1 019(18)	4 058(14)
C(32)	−1 761(20)	6 482(16)	1 370(12)	C(224)	−648(25)	1 824(19)	3 948(15)
C(33)	777(20)	7 182(17)	741(14)	C(225)	−7(18)	2 827(15)	3 597(12)
C(34)	−339(17)	7 610(17)	3 039(14)	C(226)	1 281(18)	2 966(15)	3 403(12)
C(1)	5 983(20)	6 975(21)	2 980(18)	C(331)	3 956(24)	3 828(20)	1 724(16)
C(2)	5 834(24)	9 097(18)	4 181(17)	C(332)	4 304(31)	3 365(24)	936(19)
C(3)	3 669(22)	4 789(18)	3 591(13)	C(333)	3 354(21)	2 323(17)	413(14)
O(11)	−1 919(15)	3 848(12)	1 829(10)	C(334)	2 101(25)	1 976(21)	623(16)
O(12)	1 541(16)	4 985(14)	500(9)	C(335)	1 748(22)	2 510(17)	1 386(13)
O(13)	399(17)	5 928(12)	4 340(10)	C(336)	2 666(18)	3 453(14)	1 942(11)
O(21)	4 083(17)	7 211(17)	983(11)	C(1A)	7 160(29)	750(30)	1 756(23)
O(22)	2 207(13)	8 629(11)	4 450(8)	O(1A)	6 849(31)	−265(26)	1 875(21)
O(23)	3 899(20)	10 283(14)	2 496(14)	O(1B)	6 847(28)	518(24)	51(19)
O(31)	172(24)	9 720(16)	1 572(13)				

Table 4 Fractional atomic coordinates for $[Os_3(\mu\text{-H})(CO)_{10}(o\text{-}Me_2SiC_6H_4CH_2PPh_2)]$ with standard deviations in parentheses

Atom	x	y	z	Atom	x	y	z
Os(1)	454(1)	5 576(1)	7 674(1)	O(33)	1 340(11)	5 221(7)	10 209(8)
Os(2)	3 270(1)	5 598(1)	8 291(1)	O(34)	2 577(12)	3 793(6)	7 113(7)
Os(3)	1 731(1)	4 468(1)	8 640(1)	C(1)	5 507(16)	6 564(10)	7 352(15)
P	−128(3)	6 450(2)	6 708(2)	C(2)	4 531(19)	7 332(10)	8 672(11)
Si	4 039(4)	6 682(2)	7 852(3)	C(3)	2 718(16)	7 152(8)	7 152(10)
C(11)	749(15)	5 042(9)	3 737(11)	C(111)	776(14)	6 309(8)	5 241(10)
C(12)	−1 141(17)	5 174(8)	7 693(11)	C(112)	1 661(16)	6 322(9)	4 688(11)
C(13)	198(15)	6 081(10)	8 639(10)	C(113)	2 872(19)	6 601(10)	4 955(13)
C(21)	4 833(16)	5 304(9)	8 821(11)	C(114)	3 114(16)	6 872(9)	5 729(11)
C(22)	3 683(13)	5 270(8)	7 272(9)	C(115)	2 277(13)	6 850(7)	6 307(8)
C(23)	3 055(15)	6 075(8)	9 279(11)	C(116)	1 076(13)	6 571(7)	6 032(9)
C(31)	2 980(15)	3 946(8)	9 336(11)	C(221)	−1 321(15)	7 301(9)	7 654(10)
C(32)	292(18)	3 892(8)	8 622(9)	C(222)	−1 774(17)	7 898(10)	7 939(12)
C(33)	1 480(15)	4 968(9)	9 600(10)	C(223)	−1 354(18)	8 484(11)	7 625(12)
C(34)	2 227(14)	4 076(7)	7 665(10)	C(224)	−566(17)	8 472(10)	7 063(11)
O(11)	898(12)	4 737(7)	6 159(7)	C(225)	−116(16)	7 868(9)	6 778(11)
O(12)	−2 137(12)	4 975(8)	7 734(9)	C(226)	−507(12)	7 268(7)	7 095(8)
O(13)	78(14)	6 391(8)	9 200(8)	C(331)	−2 053(14)	5 672(8)	5 794(10)
O(21)	5 813(12)	5 121(8)	9 126(8)	C(332)	−3 102(17)	5 557(10)	5 213(12)
O(22)	3 977(13)	5 093(7)	6 674(8)	C(333)	−3 734(19)	6 100(10)	4 816(12)
O(23)	2 994(14)	6 367(8)	9 881(8)	C(334)	−3 317(18)	6 732(11)	4 984(12)
O(31)	3 691(16)	3 636(8)	9 725(8)	C(335)	−2 236(16)	6 833(9)	5 570(10)
O(32)	−507(15)	3 507(8)	8 638(10)	C(336)	−1 582(12)	6 294(7)	5 979(9)

for **5** and δ −12.63, −11.86 and −8.00 for **6**. Although these are at somewhat lower fields from the range of δ −15 to −23 reported for bridging hydrides, similar values have been observed for bridging hydrides of unsaturated clusters[12] such as that at δ −11.73 for $[Os_3(\mu\text{-H})_2(CO)_{10}]$. As the hydrides at δ −12.70 for **5** and at δ −12.63 for **6** are coupled to ^{31}P to give a doublet in each case, these have been assigned to the hydride bridging the same Os–Os edge as do the bidentate ligands. The remaining pairs of hydrides at δ −11.62 and −7.89 for **5** at δ −11.86 and −8.00 for **6** have been assigned to those doubly bridging the Os–Os edge containing the Si atom at one end of the edge. The $^{31}P\text{-}\{^1H\}$ NMR resonances are observed at δ −3.50 for **5** and at δ −4.17 for **6**.

Structure of $[Os_3(\mu\text{-H})(CO)_8(o\text{-}Me_2SiC_6H_4CH_2PPh_2)]$ **5**.—The molecular structure of cluster **5** is shown in Fig. 4, the atomic coordinates are given in Table 9 and relevant bond lengths and angles in Table 10. The three Os–Os bond lengths are 3.000(2), 2.831(2) and 2.705(2) Å, with the last two being shorter than the average Os–Os bond in $[Os_3(CO)_{12}]$. The shortest Os–Os bond is most likely that containing the doubly bridged hydrides. The Os(2)–Si bond length of 2.432(6) Å is shorter than that in **2** but comparable to that in $[Os_3(\mu\text{-H})_3(CO)_9(SiPh_3)]$[11] [2.429(2) Å]. The shorter Os–Si and Os–P may be due to the unsaturated nature of this cluster. The Os(2)–Os(1)–P bond angle is 105.8(1)° and that of Os(1)–Os(2)–Si is 101.5(1)° which are like those in **1** and **2**, somewhat smaller than those in the cluster $[Os_3(\mu\text{-H})(CO)_{10}\{Si(OEt)_3\}(dppe)]$,[7] presumably due to greater strain imposed by a chelating ligand.

The sp^3 hybridisation of the silicon and phosphorus are largely preserved. The Os(2)–Si–C angles range between 111.7(6) and 115.4(9)°. The eight carbonyls are essentially linear

Table 5 Fractional atomic coordinates for $[Os_3(\mu\text{-}H)(CO)_{10}(o\text{-}HMeSiC_6H_4CH_2PPh_2)]$ with standard deviations in parentheses

Atom	x	y	z	Atom	x	y	z
Os(1)	3 472(1)	6 620(1)	1 776(1)	O(33)	1 785(23)	8 754(18)	−335(17)
Os(2)	5 970(1)	8 763(1)	3 563(1)	O(34)	5 583(21)	8 649(17)	273(15)
Os(3)	4 181(1)	9 086(1)	1 682(1)	C(1)	4 693(20)	4 966(16)	3 452(15)
P	3 161(5)	4 857(4)	2 367(4)	C(2)	8 945(27)	8 815(23)	5 716(20)
Si	7 106(6)	7 801(5)	4 687(5)	C(111)	8 260(27)	6 870(22)	3 529(19)
C(11)	1 989(23)	5 950(16)	396(20)	C(112)	8 324(32)	6 059(25)	2 861(22)
C(12)	2 256(20)	6 783(17)	2 349(17)	C(113)	7 283(25)	4 939(21)	2 369(18)
C(13)	4 730(18)	6 462(15)	1 178(16)	C(114)	6 026(24)	4 594(20)	2 530(17)
C(21)	7 284(22)	10 335(18)	4 400(17)	C(115)	6 013(22)	5 396(18)	3 257(16)
C(22)	5 005(19)	8 631(17)	4 436(21)	C(116)	7 115(21)	6 611(17)	3 776(15)
C(23)	7 111(18)	8 859(19)	2 824(15)	C(221)	2 201(22)	3 392(19)	262(16)
C(31)	3 333(24)	9 260(22)	2 578(26)	C(222)	1 678(25)	2 337(21)	−512(20)
C(32)	5 338(28)	10 740(21)	2 083(22)	C(223)	1 555(24)	1 349(21)	−102(18)
C(33)	2 656(28)	8 856(22)	430(19)	C(224)	1 813(22)	1 348(19)	940(16)
C(34)	5 127(23)	8 780(20)	854(20)	C(225)	2 299(22)	2 401(18)	1 695(17)
O(11)	1 112(20)	5 603(17)	−466(14)	C(226)	2 487(19)	3 463(16)	1 355(14)
O(12)	1 519(17)	6 827(15)	2 674(14)	C(331)	2 289(24)	5 097(19)	4 075(17)
O(13)	5 323(18)	6 309(14)	711(13)	C(332)	1 419(26)	4 842(21)	4 516(20)
O(21)	8 096(17)	11 299(14)	4 899(14)	C(333)	122(27)	3 924(21)	3 916(19)
O(22)	4 410(18)	8 454(15)	5 002(12)	C(334)	−334(31)	3 310(24)	2 849(22)
O(23)	7 856(17)	8 978(14)	2 439(12)	C(335)	634(23)	3 604(19)	2 419(18)
O(31)	2 831(19)	9 527(16)	3 114(16)	C(336)	1 938(19)	4 439(15)	3 011(14)
O(32)	6 030(22)	11 774(14)	2 314(17)				

Table 6 Relevant bond distances (Å) and angles (°) for $[Os_3(\mu\text{-}H)(CO)_{10}(o\text{-}Ph_2PC_6H_4CH_2SiMe_2)]$ **1**

Os(1)–Os(2)	3.024(1)	Mean P–C	1.82
Os(1)–Os(3)	2.915(1)	Mean Si–C	1.89
Os(2)–Os(3)	2.884(1)	Mean Os–CO	1.91
Os(1)–P	2.360(3)	Mean C–O	1.14
Os(2)–Si	2.444(4)		
Os(1)–Os(2)–Os(3)	59.2(1)	Os(3)–Os(1)–P	165.2(1)
Os(1)–Os(3)–Os(2)	62.9(1)	Os(3)–Os(2)–Si	165.1(1)
Os(2)–Os(1)–Os(3)	58.1(1)	Mean Os(1)–P–C	114.8
Os(2)–Os(1)–P	111.0(1)	Mean Os(2)–Si–C	113.0
Os(1)–Os(2)–Si	106.1(1)	Mean Os–C–O	176.3

Table 7 Relevant bond distances (Å) and angles (°) for $[Os_3(\mu\text{-}H)(CO)_{10}(o\text{-}Me_2SiC_6H_4CH_2PPh_2)]$ **2**

Os(1)–Os(2)	3.019(1)	Mean P–C	1.79
Os(1)–Os(3)	2.898(1)	Mean Si–C	1.91
Os(2)–Os(3)	2.885(1)	Mean Os–CO	1.92
Os(1)–P	2.354(5)	Mean C–O	1.13
Os(2)–Si	2.453(5)		
Os(1)–Os(2)–Os(3)	58.7(1)	Os(3)–Os(1)–P	167.3(1)
Os(1)–Os(3)–Os(2)	62.9(1)	Os(3)–Os(2)–Si	158.8(1)
Os(2)–Os(1)–Os(3)	58.3(1)	Mean Os(1)–P–C	115.2
Os(2)–Os(1)–P	109.7(1)	Mean Os(2)–Si–C	110.1
Os(1)–Os(2)–Si	102.9(1)	Mean Os–C–O	175.5

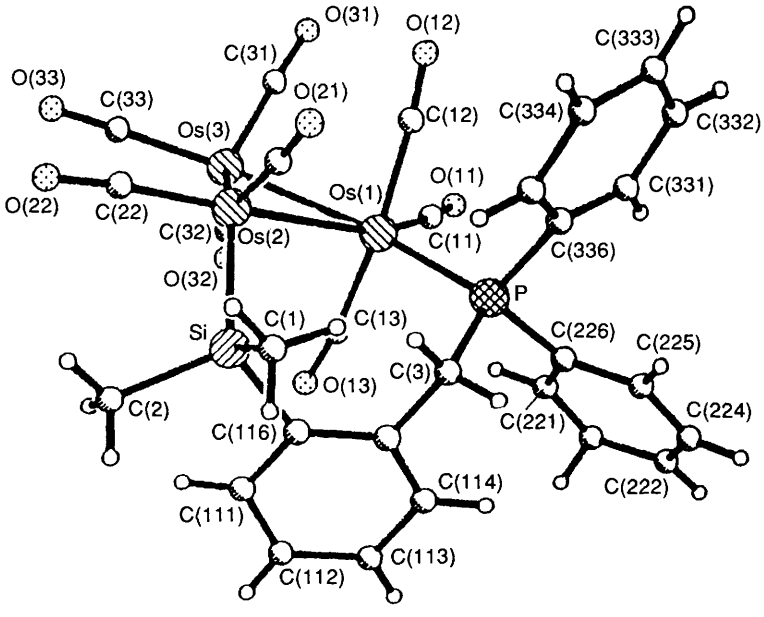

Fig. 4 The molecular structure of $[Os_3(\mu\text{-}H)_3(CO)_8(o\text{-}Me_2SiC_6H_4CH_2PPh_2)]$ **5** showing the atom labelling

(mean Os–C–O 175.7°). The Os–CO bond lengths lie between 1.842(22) and 1.929(25) Å while the C–O bond lengths range between 1.048(35) and 1.193(33) Å.

HPLC Separation of Clusters.—Complete separation of the clusters $[Os_3(CO)_{12}]$, $[Os_3(CO)_{11}(MeCN)]$, $[Os_3(CO)_{10}(MeCN)_2]$, **1**, **2** and **4** was achieved under reversed-phase conditions, using a C_{18} column and a mobile phase of 95% acetonitrile and 5% water at a flow rate of 0.5 cm^3 min^{-1}. The chromatogram is displayed in Fig. 5. The retention times (t_R),

area/height ratios, capacity factors (k') and numbers of theoretical plates (N) of the six clusters are given in Table 12. The k' values fall within the optimum range of $1 < k' < 20$.[12] The N values, ranging between 13 000 and 15 000, are comparable to the expected value of 12 500 for a well packed column of the given specifications.[13]

The elution order of the three clusters $[Os_3(CO)_{10}(MeCN)_2]$, $[Os_3(CO)_{11}(MeCN)]$ and $[Os_3(CO)_{12}]$ as previously reported[14–16] is in agreement with their relative polarities.[17] It had been suggested that the solubilities of these clusters in the mobile phase is the dominant factor influencing the elution order. Clusters **1**, **2** and **4** are eluted after $[Os_3(CO)_{12}]$, $[Os_3(CO)_{11}(MeCN)]$ and $[Os_3(CO)_{10}(MeCN)_2]$ as they are of significantly higher molecular weights, with **4** (the cluster of lower molecular weight) being eluted first: **1** and **2** have the same molecular weight, but **2** is eluted before **1**. The dominant factor which influences the chromatographic behaviour of these clusters is likely to be the relative solubilities of the two clusters in the mobile phase.

Clusters **1**, **2** and **4** differ in the substituent groups on the silicon and phosphorus donor atoms of the ligands. The nature of these substituent groups influences the chromatographic behaviour of these clusters, and enables them to be effectively separated.

The spectral overlay plots are displayed in Fig. 6. The ratio plot of the signals at 230 and 254 nm is given in Fig. 7. These plots show that a good separation of all six compounds has been achieved, as they are characterised by well matched spectral overlays and fairly constant ratio plots (see Experimental section).

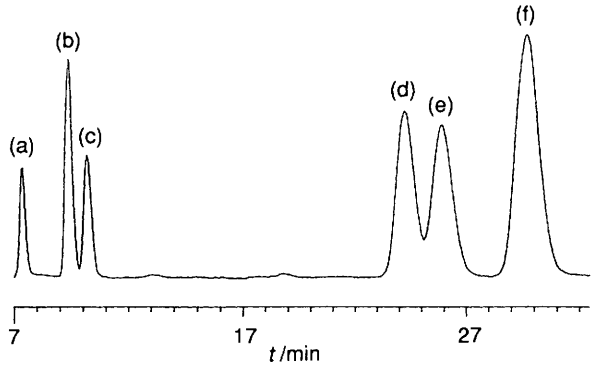

Fig. 5 Reversed-phase HPLC chromatogram. From left: (a) $[Os_3(CO)_{10}(MeCN)_2]$, (b) $[Os_3(CO)_{11}(MeCN)]$, (c) $[Os_3(CO)_{12}]$, (d) **4**, (e) **2** and (f) **1**. Mobile phase: 95% acetonitrile and 5% water. Column: LiChrospher 100 CH-18/2, 250 × 4 mm, 10 μm. Flow rate: 0.5 cm^3 min^{-1}

Experimental

All reactions were carried out in evacuated reaction tubes. All solvents were dried over appropriate drying agents and distilled before use. Infrared spectra were recorded on a Perkin-Elmer model 983G spectrophotometer, ^1H, ^{31}P and ^{29}Si NMR spectra on a JEOL FX-90Q FT instrument using $SiMe_4$ (^1H and ^{29}Si) or H_3PO_4 (^{31}P) as reference. The products of the reactions were separated by thin-layer chromatography on 20 × 20 cm glass plates coated with 0.5 mm of Merck Kieselgel 60 GF, using mixtures of dichloromethane and hexane in various proportions as eluents.

Table 8 Relevant bond distances (Å) and angles (°) for $[Os_3(\mu\text{-H})(CO)_{10}(o\text{-HMeSiC}_6H_4CH_2PPh_2)]$ **4**

Os(1)–Os(2)	3.036(1)	Mean P–C	1.84
Os(1)–Os(3)	2.907(1)	Mean Si–C	1.88
Os(2)–Os(3)	2.884(1)	Mean Os–CO	1.90
Os(1)–P	2.363(5)	Mean C–O	1.14
Os(2)–Si	2.425(7)		
Os(1)–Os(2)–Os(3)	58.8(1)	Os(3)–Os(1)–P	164.4(1)
Os(1)–Os(3)–Os(2)	63.2(1)	Os(3)–Os(2)–Si	159.5(1)
Os(2)–Os(1)–Os(3)	58.0(1)	Mean Os(1)–P–C	115.5
Os(2)–Os(1)–P	108.5(1)	Mean Os(2)–Si–C	112.6
Os(1)–Os(2)–Si	102.1(1)	Mean Os–C–O	175.2

Table 10 Relevant bond distances (Å) and angles (°) for $[Os_3(\mu\text{-H})(CO)_8(o\text{-Me}_2SiC_6H_4CH_2PPh_2)]$ **5**

Os(1)–Os(2)	3.000(2)	Mean P–C	1.82
Os(1)–Os(3)	2.831(2)	Mean Si–C	1.90
Os(2)–Os(3)	2.705(2)	Mean Os–CO	1.89
Os(1)–P	2.334(5)	Mean C–O	1.13
Os(2)–Si	2.432(6)		
Os(1)–Os(2)–Os(3)	59.2(1)	Os(3)–Os(1)–P	160.9(1)
Os(1)–Os(3)–Os(2)	65.6(1)	Os(3)–Os(2)–Si	135.0(1)
Os(2)–Os(1)–Os(3)	55.2(1)	Mean Os(1)–P–C	115.0
Os(2)–Os(1)–P	105.8(1)	Mean Os(2)–Si–C	113.0
Os(1)–Os(2)–Si	101.5(1)	Mean Os–C–O	175.7

Table 9 Fractional atomic coordinates for $[Os_3(\mu\text{-H})_3(CO)_8(o\text{-Me}_2SiC_6H_4CH_2PPh_2)]$ with standard deviations in parentheses

Atom	x	y	z	Atom	x	y	z
Os(1)	1900(1)	3142(1)	346(1)	C(1)	3770(24)	305(22)	2017(12)
Os(2)	2249(1)	823(1)	457(1)	C(2)	5033(20)	−294(17)	961(14)
Os(3)	1678(1)	1730(1)	−675(1)	C(3)	3426(18)	3007(16)	1839(8)
Si	3985(5)	723(4)	1202(3)	C(111)	5827(20)	2033(17)	928(11)
P	2304(4)	3801(4)	1361(2)	C(112)	6564(22)	2877(19)	994(11)
C(11)	1400(22)	4367(22)	−91(10)	C(113)	6271(22)	3789(21)	1296(12)
C(12)	330(19)	2820(19)	446(11)	C(114)	5244(21)	3779(20)	1599(12)
C(13)	3427(21)	3378(17)	145(10)	C(115)	4521(17)	2947(15)	1551(9)
C(21)	1515(21)	448(19)	1131(11)	C(116)	4811(18)	2026(15)	1259(10)
C(22)	2414(18)	−579(17)	293(11)	C(221)	3266(21)	5683(19)	1073(12)
C(31)	286(22)	2305(29)	−990(12)	C(222)	3766(27)	6665(22)	1154(14)
C(32)	2494(20)	2640(22)	−1180(9)	C(223)	3769(23)	7090(20)	1763(12)
C(33)	1629(20)	540(20)	−1222(12)	C(224)	3315(23)	6562(22)	2202(13)
O(11)	1102(19)	5068(17)	−406(9)	C(225)	2839(18)	5601(17)	2082(10)
O(12)	−545(15)	2563(14)	508(10)	C(226)	2811(19)	5108(17)	1495(10)
O(13)	4264(15)	3485(15)	−48(8)	C(331)	351(21)	4504(20)	1789(11)
O(21)	1005(15)	208(16)	1526(8)	C(332)	−692(22)	4423(20)	2044(12)
O(22)	2592(18)	−1417(16)	198(10)	C(333)	−975(23)	3455(19)	2307(12)
O(31)	−615(16)	2682(18)	−1192(9)	C(334)	−170(24)	2643(23)	2335(13)
O(32)	2896(22)	3127(20)	−1477(10)	C(335)	870(23)	2769(21)	2065(12)
O(33)	1620(16)	−144(15)	−1551(9)	C(336)	1090(15)	3708(14)	1803(8)

Table 11 Crystal data and details of measurements for the complexes

	1	2	4	5
Formula	$C_{31}H_{22}O_{11}Os_3PSi$	$C_{31}H_{22}O_{10}Os_3PSi$	$C_{30}H_{20}O_{10}Os_3PSi$	$C_{29}H_{22}O_8Os_3PSi$
M	1184.1	1234.2	1168.1	1128.1
Crystal symmetry	Monoclinic	Triclinic	Triclinic	Monoclinic
Space group	$P2_1/n$	$P\bar{1}$	$P\bar{1}$	$P2_1/c$
a/Å	10.685(2)	10.497(2)	11.834(2)	11.748(6)
b/Å	19.797(3)	12.306(3)	12.693(2)	12.790(8)
c/Å	16.332(3)	15.150(4)	13.561(2)	21.534(9)
α/°		95.270(1)	94.640(1)	
β/°	98.780(3)	97.440(2)	110.270(2)	97.330(2)
γ/°		105.600(1)	114.870(2)	
U/Å^3	3414.2(10)	1852.7(8)	1670.9(5)	3209(3)
Z	4	2	2	4
$F(000)$	2180	1146	1070	2068
D_c/g cm^{-3}	2.304	2.212	2.322	2.335
μ(Mo-Kα)/cm^{-1}	112.87	104.08	115.29	119.98
Measured reflections	6549	8548	6141	6148
Independent reflections	5999	8127	5840	5575
Observed reflections [$F > 6.0\sigma(F)$]	3825	5246	3270	3717
Absorption correction (minimum, maximum)	0.1147, 0.2310	0.1384, 0.2306	0.4147, 0.9567	0.2266, 0.9682
R	0.0443	0.0659	0.0458	0.0638
R'*	0.0647	0.0948	0.0560	0.0871
g	0.0068	0.0029	0.0016	0.0055
Goodness of fit	0.72	0.18	0.99	1.04

* Weighting scheme $w^{-1} = \sigma^2(F) + |g|F^2$.

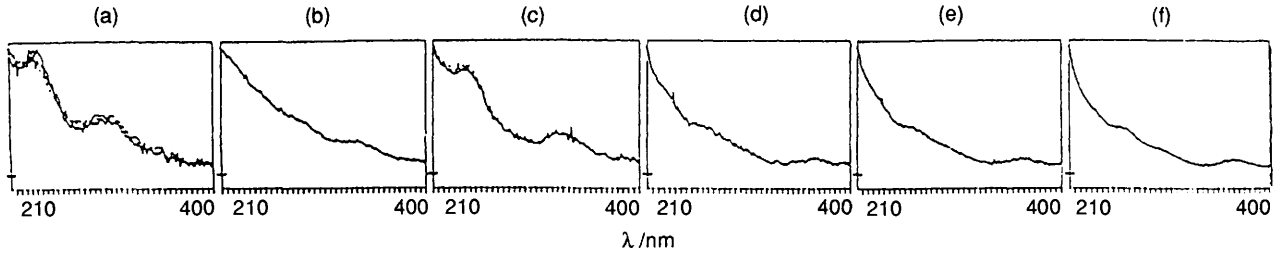

Fig. 6 Ultraviolet absorption spectra (211–401 nm) for clusters between the time intervals, in minutes, shown within parentheses, using the photodiode-array detector. From left: (a) $[Os_3(CO)_{10}(MeCN)_2]$ (6.74–7.03), (b) $[Os_3(CO)_{11}(MeCN)]$ (8.72–9.02), (c) $[Os_3(CO)_{12}]$ (9.52–9.87), (d) **4** (23.38–24.17), (e) **2** (25.02–25.86) and (f) **1** (28.69–29.64). Other details as in Fig. 5

X-Ray Structural Determination.—Crystal data and details of measurements for complexes **1**, **2**, **4** and **5** are reported in Table 11. Diffraction intensities were collected at 298 K on a Siemens R3m/V X-ray diffractometer, ω–2θ scan mode with graphite-monochromatised Mo-Kα radiation (λ = 0.710 69 Å), scan range 1.3°, scan speed 3.5–15° min^{-1} and $3.0 < 2\theta < 50.0°$, $+h$, $+k$, $\pm l$ for **1** and **5** and $+h$, $\pm k$, $\pm l$ for **2** and **4**. All computations were carried out on a MicroVAX 2000 computer using the SHELXTL PLUS program package.[18] The structures were solved by direct methods for the osmium atoms, and Fourier difference techniques for the remaining non-hydrogen atoms. Full-matrix, least-squares refinement with all non-hydrogen atoms anisotropic and hydrogen atoms in calculated position. An empirical (ψ-scan) correction was performed in each case.

Additional material available from the Cambridge Crystallographic Data Centre comprises H-atom coordinates, thermal parameters and remaining bond lengths and angles.

Synthesis of o-$Ph_2PC_6H_4CH_2SiMe_2H$ **I** *and* o-HMe_2Si-$C_6H_4CH_2PPh_2$ **II**.—(o-Bromobenzyl)dimethylsilane (34.55 g, 0.14 mmol), in dry diethyl ether (*ca.* 200 cm^3) was added dropwise to magnesium turnings (3.66 g, 0.15 mmol) suspended in ether. The resulting reaction mixture was refluxed at 50 °C for 3 h. Chlorodiphenylphosphine (33.10 g, 0.15 mmol) was added dropwise to the cooled reaction mixture which was left to be stirred overnight. Saturated ammonium chloride solution was added slowly until a clear aqueous layer was observed to form below the ether layer. The ether layer was dried overnight with anhydrous sodium sulfate. Bulb-to-bulb distillation of the colourless liquid yielded a heavy liquid (17.66 g) at 0.01 mmHg and an external bath temperature of 175–180 °C (Found: C, 75.45; H, 6.90; P, 9.35. Calc. for $C_{21}H_{23}PSi$: C, 75.45; H, 6.90; P, 9.30%).

Synthesis of o-$Ph_2PC_6H_4CH_2SiMeH_2$ **III** *and* o-H_2MeSi-$C_6H_4CH_2PPh_2$ **IV**.—(o-Bromobenzyl)methylsilane (24.63 g, 0.11 mmol) in dry diethyl ether (*ca.* 150 cm^3) was added dropwise to magnesium turnings (3.00 g, 0.12 mmol) also suspended in ether. The reaction mixture was refluxed at 50 °C for 3 h. An ether solution of chlorodiphenylphosphine (31.5 g, 0.14 mmol) was next slowly added to give a yellow solution which was stirred overnight under nitrogen. The excess of Grignard reagent was hydrolysed by a saturated solution of ammonium chloride. The ether layer was dried over anhydrous sodium sulfate. Bulb-to-bulb distillation of the remaining liquid after removal of ether yielded a heavy, colourless liquid (2.6 g) at 0.01 mmHg and an external bath temperature of 175–180 °C (Found: C, 74.90; H, 6.50; P, 9.90. Calc. for $C_{20}H_{21}PSi$: C, 75.00; H, 6.55; P, 9.70%).

Reaction of o-$Ph_2PC_6H_4CH_2SiMe_2H$ *and* o-HMe_2Si-$C_6H_4CH_2PPh_2$ *with* $[Os_3(CO)_{10}(MeCN)_2]$.—A CH_2Cl_2 solution containing o-$Ph_2PC_6H_4CH_2SiMe_2H$ and o-HMe_2Si-$C_6H_4CH_2PPh_2$ (29 mg, 0.08 mmol) was added to $[Os_3(CO)_{10}$-$(MeCN)_2]$ (60 mg, 0.06 mmol) dissolved in CH_2Cl_2 (5 cm^3) in a

Table 12 Chromatographic data (a) $[Os_3(CO)_{10}(MeCN)_2]$, (b) $[Os_3(CO)_{11}(MeCN)]$, (c) $[Os_3(CO)_{12}]$, (d) **4**, (e) **2** and (f) **1**

Cluster*	t_R/min	V_R/cm^3	Area/Height	k'	N
(a)	6.88	3.44	0.300	1.991	13 218
(b)	8.88	4.44	0.362	2.861	15 123
(c)	9.69	4.84	0.399	3.213	14 823
(d)	23.77	11.88	0.971	9.335	15 061
(e)	25.41	12.70	1.080	10.048	13 912
(f)	29.18	14.59	1.202	11.687	14 812

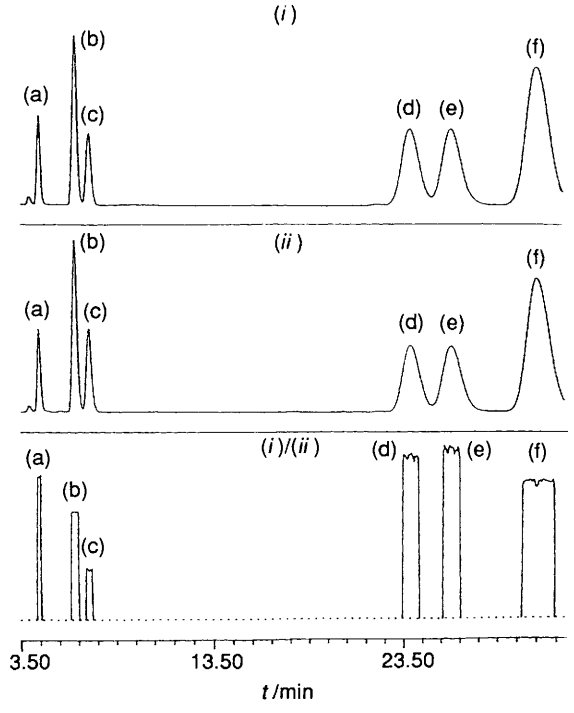

Fig. 7 Ratio plots (*i*)/(*ii*) signals at 230 nm (*i*) to those at 254 nm (*ii*). Details as in Fig. 5

reaction tube which was then evacuated. The reaction mixture was stirred at room temperature for 24 h to give an orange-brown solution. The concentrated solution was subjected to TLC using dichloromethane–hexane (1:9) as the eluent, giving two yellow bands. Compound **1** was extracted from the band of $R_f = 0.26$, and **2** from that of $R_f = 0.18$. Diffraction-quality crystals of **1** and **2** were obtained upon recrystallisation from CH_2Cl_2 and a mixture of dichloromethane and hexane respectively (Found: C, 31.05; H, 1.95; P, 2.55. Calc. for $C_{31}H_{23}O_{10}Os_3PSi$: C, 31.40; H, 1.95; P, 2.60%).

Reaction of o-$Ph_2PC_6H_4CH_2SiMeH_2$ *and* o-$H_2MeSiC_6H_4CH_2PPh_2$ *with* $[Os_3(CO)_{10}(MeCN)_2]$.—A CH_2Cl_2 solution containing o-$Ph_2PC_6H_4CH_2SiMeH_2$ and $Ph_2PCH_2C_6H_4SiMeH_2$-o was added to a solution of $[Os_3(CO)_{10}(MeCN)_2]$ (100 mg, 0.11 mmol) in a reaction tube which was then evacuated. After nearly 20 h of stirring the reaction mixture turned intensely orange. Thin-layer chromatography using as eluent dichloromethane–hexane (1:4) gave a major band (R_f 0.38) from which **4** was recovered, and further recrystallisation from a mixture of dichloromethane and hexane yielded diffraction-quality crystals. Compound **3** was recovered as the minor product and was found to decompose rapidly in air (Found: C, 30.75; H, 1.55; P, 2.50. Calc. for $C_{30}H_{21}O_{10}Os_3PSi$: C, 30.75; H, 1.80; P, 2.65%).

Reaction of o-$Ph_2PC_6H_4CH_2SiMe_2H$ *and* o-$HMe_2SiC_6H_4CH_2PPh_2$ *with* $[Os_3H_2(CO)_{10}]$.—A CH_2Cl_2 solution of o-$Ph_2PC_6H_4CH_2SiMe_2H$ and o-$HMe_2SiC_6H_4CH_2PPh_2$ was added to $[Os_3H_2(CO)_{10}]$ (100 mg, 0.12 mmol) in a reaction tube which was evacuated. The reaction mixture was stirred for 24 h at room temperature during which time it turned from purple to yellow, then to orange. Thin-layer chromatography, using an eluent of dichloromethane–hexane (3:7), led to a major band (R_f 0.35) identified as $[Os_3(\mu\text{-}H)(CO)_{10}(o\text{-}Me_2SiC_6H_4CH_2PPh_2)]$. The minor band at a R_f value of 0.50 gave $[Os_3(\mu\text{-}H)_3(CO)_8(o\text{-}Me_2SiC_6H_4CH_2PPh_2)]$ (Found: C, 30.75; H, 2.10; P, 2.70. Calc. for $C_{29}H_{25}O_8Os_3PSi$: C, 30.80; H, 2.20; P, 2.75%).

Reaction of o-$Ph_2PC_6H_4CH_2SiMeH_2$ *and* o-$H_2MeSiC_6H_4CH_2PPh_2$ *with* $[Os_3(\mu\text{-}H)_2(CO)_{10}]$.—The cluster $[Os_3H_2(CO)_{10}]$ (60 mg, 0.07 mmol) was allowed to react with a CH_2Cl_2 solution of o-$Ph_2PC_6H_4CH_2SiMeH_2$ and o-$H_2MeSiC_6H_4CH_2PPh_2$ (29 mg, 0.09 mmol) in an evacuated reaction tube. After stirring for 24 h at room temperature the orange solution formed was concentrated and subjected to TLC using CH_2Cl_2–hexane (1:4) as eluent. This gave a major band of $R_f = 0.38$ from which $[Os_3(\mu\text{-}H)(CO)_{10}(o\text{-}HMeSiC_6H_4CH_2PPh_2)]$ was recovered. A second product **6** eluted at $R_f = 0.50$ was formulated as $[Os_3(\mu\text{-}H)_3(CO)_8(o\text{-}HMeSiC_6H_4CH_2PPh_2)]$ on the basis of its IR and ^1H and ^{31}P NMR spectral data.

HPLC Separation.—The HPLC separations of the osmium clusters were undertaken using a Hewlett-Packard HP1090 liquid chromatograph equipped with a HP-85B personal computer, 3392A integrator and a 1040A diode-array detector. The reversed-phase column (250 × 4 mm internal diameter) used contained LiChrospher 100 CH-18/2, 10 μm. The mobile phases ranged from 100% acetonitrile to mixtures of acetonitrile and methanol, at a flow rate of 0.5 cm^3 min^{-1}. The temperature in all the runs was 35 °C. All solvents were of HPLC grade and were filtered and degassed in helium prior to use. Samples were dissolved in premixed mobile phases filtered through a 0.45 μm pore filter and injected in 5 μl volumes with a Rheodyne model 7010 injector. The column dead volume in each separation was determined with reference to the first baseline peak which appeared on injection.[19]

The identities of all the chromatographic peaks were established as follows: (*a*) the absorption spectra of the individual osmium clusters were first obtained using a Perkin-Elmer Lambda 9 UV/VIS/NIR spectrophotometer; (*b*) the absorption spectra of the eluents at specific times corresponding to the peak maxima were determined using the diode-array detector and an evaluation program of the Data Evaluation Pack software of the HP-85B computer; and (*c*) the resultant spectra were compared with the individual spectra of the compounds, confirming their identities.

The purity of all the observed chromatographic peaks was further checked through (1) overlay of the absorption spectra at three different points (upslope, apex and downslope) of each peak, and (2) determination of the ratio of the heights of the chromatographic peaks monitored at two specific wavelengths (230 and 254 nm). Again, the diode-array detector and the evaluation program (Data Evaluation Pack) of the HP1090 liquid chromatograph were applied. For a pure chromatographic peak the spectral overlay should match, and the ratio of the two signals across a peak elution profile should remain fairly constant. Using these methods, many of the chromatographic peaks obtained from the separations were found to correspond to pure triosmium cluster compounds.

References

1 A. J. Deeming, S. Donovan-Mtunzi and S. E. Kabir, *J. Organomet. Chem.*, 1987, **333**, 253.
2 A. J. Deeming, S. Donovan-Mtunzi, K. I. Hardcastle, S. E. Kabir, K. Henrick and M. McPartlin, *J. Chem. Soc., Dalton Trans.*, 1988, 579.

3 F. W. B. Einstein, R. K. Pomeroy and A. C. Willis, *J. Organomet. Chem.*, 1986, **311**, 257.
4 A. C. Willis, F. W. B. Einstein, R. M. Ramadan and R. K. Pomeroy, *Organometallics*, 1983, 935.
5 B. F. G. Johnson, J. Lewis and M. Monari, *J. Chem. Soc., Dalton Trans.*, 1990, 3525.
6 R. D. Adams, J. E. Cortopassi and M. P. Pompco, *Inorg. Chem.*, 1991, **15**, 2960.
7 B. F. G. Johnson, J. Lewis, M. Monari, D. Braga, F. Grepioni and C. Gradella, *J. Chem. Soc., Dalton Trans.*, 1990, 2863.
8 R. D. Holmes-Smith, S. R. Stobart, R. Vefghi and M. J. Zaworotko, K. Jochem and T. S. Cameron, *J. Chem. Soc., Dalton Trans.*, 1987, 969.
9 H. J. R. de Boer, O. S. Akkerman and F. Bickelhaupt, *Angew. Chem., Int. Ed. Engl.*, 1988, **27**, 687.
10 E. A. V. Ebsworth, A. P. McIntosh and M. Schröder, *J. Organomet. Chem.*, 1986, **C41**, 312.
11 A. P. Humphries and H. D. Kaesz, *Prog. Inorg. Chem.*, 1979, **25**, 145.
12 B. L. Karger, L. R. Snyder and C. Horvath, *An Introduction to Separation Science*, Wiley, New York, 1973.
13 V. R. Meyer, *J. Chromatogr.*, 1985, **334**, 197.
14 H. G. Ang, W. K. Kwik and W. K. Leong, *J. Organomet. Chem.*, 1989, **379**, 325.
15 H. G. Ang, W. L. Kwik and E. Morrison, *J. Fluorine Chem.*, 1991, **51**, 83.
16 H. G. Ang, W. L. Kwik and W. K. Leong, *J. Chromatogr.*, 1991, **537**, 475.
17 L. R. Snyder and J. J. Kirkland, *Introduction to Modern Liquid Chromatography*, 2nd edn., Wiley, New York, 1979.
18 G. M. Sheldrick, SHELXTL PLUS Users Manual, Nicolet XRD Corporation, Madison, WI, 1986.
19 W. L. Hine, T. E. Riene, D. W. Armstrong, De Mond, A. Ala and T. Ward, *Anal. Chem.*, 1985, **57**, 237.

Received 12*th February* 1992; *Paper* 2/00759B